GC/MS-Based Urinary Metabolomics Reveals Systematic Differences in Metabolism and Ethanol Response between Sprague–Dawley and Wistar Rats

By: Xianfu Gao, Aihua Zhao, Mingmei Zhou, Jingchao Lin, Yunping Qiu, Mingming Su, and Wei Jia

Gao, X.F., Zhao, A.H., Zhou, M.M., Lin, J.C., Qiu, Y.P., Su, M.M., & Jia, W. (2011). GC/MS-based urinary metabolomics reveals systematic differences in metabolism and ethanol response between Sprague-Dawley and Wistar rats. *Metabolomics, 7*(3), 363-374.

Abstract:
Metabolic differences of experimental animals contribute to pharmacological variations. Sprague–Dawley (SD) and Wistar rats are commonly used experimental rats with similar genetic background, and considered interchangeable in practical researches. In this study, we present the urinary metabolomics results, based on gas chromatography coupled to mass spectrometry (GC/MS), which reveal the systematic metabolic differences between SD and Wistar rats under different perturbations such as fasting, feeding, and consecutive acute ethanol interventions. The different metabotypes between the two strains of rats involve a number of metabolic pathways and symbiotic gut microflora. SD rats exhibited higher individualized metabolic variations in the fasting and feeding states, and a stronger ability to recover from an altered metabolic profile with less hepatic injury from the consecutive ethanol exposure, as compared to Wistar rats. In summary, the GC/MS-based urinary metabolomics studies demonstrated an intrinsic metabolic difference between SD and Wistar rats, which warrants consideration in experimental design using these animal strains.

Article:
INTRODUCTION
Genetic and physiological diversity of laboratory animals produces an increasing challenge on selecting reasonable animal subjects for achieving optimum results while minimizing costs in pharmacological, toxicological, and nutritional researches. The differences of susceptibility to drugs, nutrients, and stress recently are documented between strains of commonly used experimental animals with similar genetic background. Various intrinsic physiological factors and external influences are known to affect the metabolite composition of biofluids. These intrinsic factors include species (Potts et al. 2001; Salek et al. 2007), strains and genetic modification (Holmes et al. 2000), gender (McKee et al. 2006), age (Plumb et al. 2005; Psihogios et al. 2008), physiological rhythm (Bollard et al. 2001), and inter-individual variation. Some external factors such as diurnal variation (Bollard et al. 2001; Slupsky et al. 2007), stress (Teague et al. 2007; Wang et al. 2007, 2009), and gut microflora (Wikoff et al. 2009) were investigated as well. Sprague–Dawley (SD) rats and Wistar rats are very similar strains

metabolically and genetically, and are the commonly used laboratory rodent animals. Holmes et al. (2000) applied nuclear magnetic resonance (NMR)-based metabonomics to find a partial separation of urinary profiles between Han Wistar and SD rats by principal component analysis (PCA), and observed a distinct difference of metabolic profiles between these two rats using probabilistic neural networks.

To date, the majority of such investigations were carried out using NMR-based metabonomics methodology mainly pioneered by Nicholson and coworkers (Bollard et al. 2005). However, the investigation into strain-related variations of rats was only reported between SD and Han Wistar rats by NMR-based metabonomics (Holmes et al. 2000). It is essential to explore the differences between SD and Wistar rats based on alternative technological platform, and provide complementary information to the outcomes of the NMR technology. Mass spectrometry, especially coupled with advanced chromatographic separation instruments, is a powerful tool for metabolomics studies due to its wider dynamic range, reproducible quantitative capabilities, and its ability to analyze samples of significant molecular complexity (Want et al. 2007). Gas chromatography coupled to mass spectrometry (GC/MS) was shown to be a robust method with more satisfactory sensitivity and resolution than the conventional NMR approach and better reliability in structural identification of candidate biomarkers than liquid chromatography coupled to mass spectrometry (LC/MS) (Lenz and Wilson 2007). Non-targeted GC/MS analysis has been successfully applied in metabolomics analysis on urinary, serum samples and tissue extracts (Jiye et al. 2005; Lin et al. 2008; Qiu et al. 2007).

Understanding the metabolic differences and their crucial metabolites responsible for such variations helps to increase our knowledge about strain characteristics and improve the subsequent data interpretation. The current study was designed to compare the strain-related metabolic differences in the fasting and feeding state, and the different response to the external intervention (e.g. acute ethanol exposure) between SD and Wistar rats by GC/MS-based metabolomics techniques. The stress reaction to abrupt living environmental changes and the inter-individual variation were observed as well. The physiological parameters of serum and liver tissue were simultaneously determined to support the results of metabolomics in acute ethanol intervention experiment.

MATERIALS AND METHODS

Animals

Eight-week-old male SD and Wistar rats were purchased from Shanghai Laboratory Animal Co. Ltd. (China), and housed in stainless steel standard cages in groups (five SD or Wistar rats per cage) with a certified standard rat diet and water available ad libitum. A constant 12-h light/dark cycle was maintained in an environmentally controlled breeding room with temperature 23 ± 1°C and humidity 60 ± 5%. After adaptation for 1 week, rats were grouped for the following experiments. Additionally, all rats were always housed in the same standard cages with standard rat diet and water ad libitum except as otherwise noted. Principles of laboratory animal care and all procedures are conducted in accordance with the National Guide for the Care and Use of Laboratory Animals, China. The experimental design is illustrated in Fig. 1.

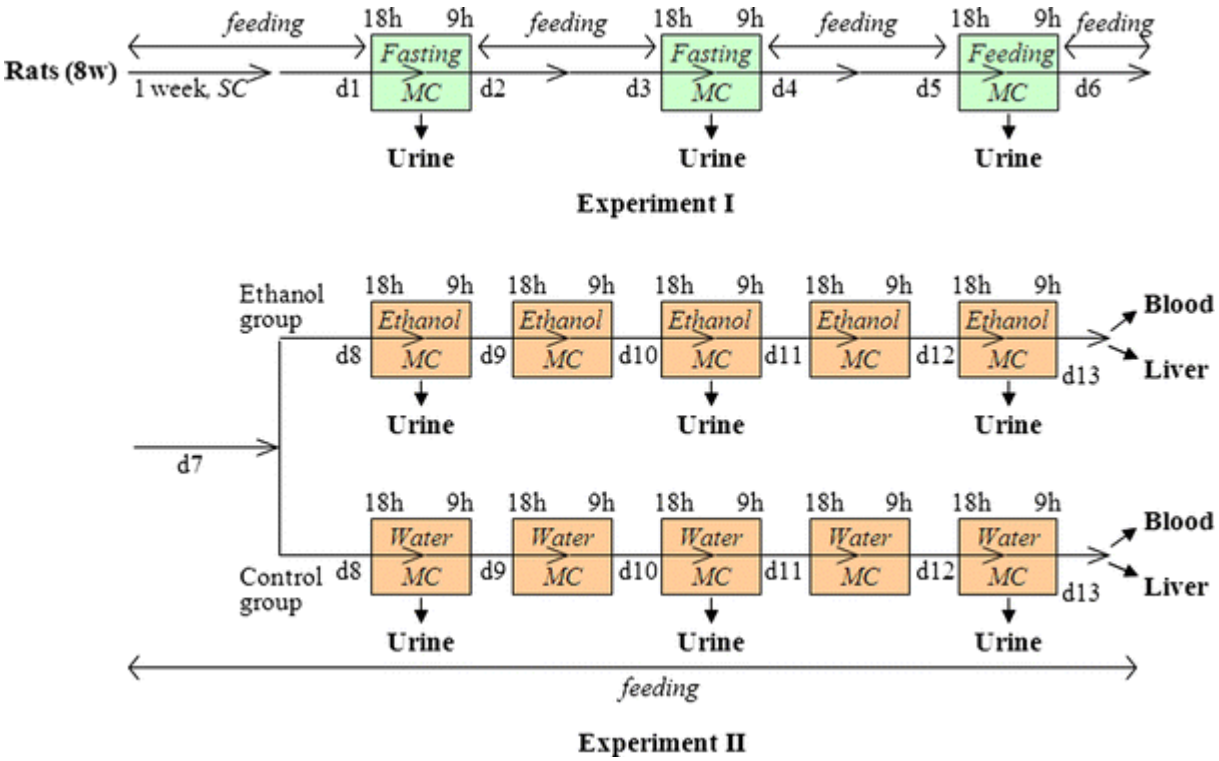

Figure 1: Flowchart of experiment designs in this study. All rats could drink water freely during the whole experiment. Key: *8 w* 8-week old, *SC* standard cage, *MC* metabolism cage; 18 h(9 h), 18:00 (9:00); *d*1(*d*2,…,*d*13), the 1st (or 2ed,…,13th) experimental day after the initial 1 week of adaption in standard cages

Experiment design I: systematic comparisons between SD and Wistar rats under fasting and feeding states. (A) Twenty rats per strain were housed individually in metabolism cages in fasting and water ad libitum from 18:00 h of day 1 (*d*1) to 9:00 h of day 2 (*d*2). The process was repeated from day 3 (*d*3) to day 4 (*d*4). Urine samples were collected for determining the nocturnal urinary metabolome of fasting rats. (B) The same SD and Wistar rats were housed in metabolic cages individually with foodstuff and water ad libitum from 18:00 h of day 5 (*d*5) to 9:00 h of day 6 (*d*6). All urine samples were collected for determining the nocturnal urinary metabolome of feeding rats.

Experiment design II: systematic comparisons between SD and Wistar rats following acute ethanol exposure. All rats after experiment I were housed in the same standard cages for another two days with food and water available ad libitum, then divided into an ethanol group and a control group. From day 8 (*d*8), 10 rats per strain were intragastrically administrated with 8 ml 50% ethanol/kg body weight for twice separated by 1 h (ethanol group), and the control group (n = 10) received the same volume of deionized water. All processes were repeated in the following 4 days (*d*9–*d*12). After ethanol or deionized water was administrated, all rats were immediately placed into individual metabolism cages, and the overnight urine samples (from 18:00h to 9:00h) were collected. All rats were sacrificed after the last urine collection (day 13), and the whole blood and liver were collected immediately.

Sample preparation and biochemical determination of serums and liver tissues

The blood samples were immediately centrifuged at 9,300 × *g* and 4°C for 15 min, and the supernatants (serum) were transferred to determine the biochemical parameters. Liver tissues were rapidly excised from the sacrificed animals and stored at –80°C. Prior to analysis, liver tissues were homogenized with ice-cold saline and subsequently the mixture was centrifuged at 9,300 × *g* and at 4°C for 15 min. The supernatants were used in the determination of liver biochemical parameters.

Serum enzyme activities, such as alanine aminotransferase (ALT), aspartate aminotransferase (AST), and lactate dehydrogenase (LDH), were analyzed on an automatic analyzer (Roche/Hitachi, Modular P800) using Roche reagents in the Clinical Biochemical Laboratory. Liver enzyme activities were determined using kits (Jiancheng Bioengineering Institute, China) as follows: Tissue protein content was analyzed by using the Protein kit. Superoxide dismutase (SOD) activity was measured using the SOD kit based on the method of xanthine oxidase. The OD value is measured at the wavelength of 550 nm after reaction at 37°C for 40 min. One unit of SOD activity is defined as the amount of enzyme that gave 50% inhibition of SOD per mg protein. Glutathione peroxidase (GSH-PX) activity was assayed using the GSH-PX kit. One unit of GSH-PX is equal to the decrease of 1 μM GSH per mg protein within 1 min. The enzyme activity is expressed as units/min/mg protein. Lipid peroxidation (LPO) of liver was determined using the malondialdehyde kit based on the formation of a red chromophore that absorbs at 532 nm. The results are expressed as nanomoles of malondialdehyde/mg protein.

Preparation of urine samples and GC/MS analysis

The urine samples after collection were immediately centrifuged at 5,900 × *g* and at 4°C for 10 min for removing any solid debris, and the supernatants were stored in aliquots at –80°C before derivatization. The derivatization of urine samples by ethyl chloroformate and GC/MS analysis were performed according to our previously published methods (Qiu et al. 2007). L-2-chlorophenylalanine, an internal standard (IS), was used to monitor GC/MS performance and method reproducibility during a long time of run.

Extraction of GC/MS data and multivariate statistical analysis

Raw GC/MS data were converted into AIA format (NetCDF) files by the Agilent GC–MS 5975 Data Analysis software, and subsequently processed by the XCMS toolbox (version 1.14.0) using the parameters as previously described (Gao et al. 2009). The XCMS output was further processed using the Microsoft Excel software (Microsoft, Redmond, WA), where the IS peaks, and impurity peaks from column bleeds and derivatization procedures were excluded, and the remaining ion features were normalized to the total integrated area (1,000) per sample and arranged on a three-dimensional matrix consisting of arbitrary peak index (rt-*m/z* pair), sample names (observations), and peak area (variables).

The resulting three-dimensional matrix was imported into the Simca-P 11.0 software package (Umetrics, Umeå, Sweden). Principle component analysis (PCA) was performed on the mean-centered and UV-scaled data to visualize general clustering, trends, and outliers among all samples on the scores plot. R^2X represents the cumulative interpretation ability of the current model, where the value close to 1 indicates an excellent model. Partial least squares discriminant analysis (PLS–DA) was performed to simultaneously profile the ethanol and control groups of

the two strains of rats. Orthogonal projections to latent structures discriminant analysis (OPLS–DA) (Bylesjö et al. 2006) was utilized to construct a predictive model and to identify the differential metabolites responsible for the strain-related differences or differences between the ethanol group and the control group. R^2Y is the cumulative model variation in Y, and Q^2Y is the cumulative predicted variation in Y. The values of these parameters approaching 1.0 indicated a stable model with a predictive reliability. The discriminating metabolites were obtained using a statistically significant threshold of variable influence on projection (VIP) values obtained from the OPLS–DA model and two-tailed Student's *t* test (*P* value) on the normalized raw data at univariate analysis level, where the metabolites with VIP values larger than 1.0 and *P* values less than 0.05 were selected. Fold change was calculated as the logarithm of the average mass response (area) ratio between two arbitrary classes, where the positive value means that the average mass response of class 1 is larger than that of class 2.

Identification of discriminating metabolites

The identification of the discriminating metabolites was firstly performed by comparing the retention time and mass spectra of each compound with those of reference standards available in our lab. The remaining metabolites were identified by searching against commercially available libraries such as NIST05. The deconvoluted mass spectra by the Automated Mass Spectral Deconvolution and Identification System (AMDIS) were transferred to the NIST Mass Spectral Search Program MS Search 2.0 for matching against the NIST Mass Spectral Library 2005.

RESULTS AND DISCUSSION

GC/MS analysis of rat urinary metabolome

All samples were prepared, derivatized, and analyzed according to our previously published method (Qiu et al. 2007). Instrumental performance and method reproducibility were monitored by an internal standard so as to ensure the reliability of GC/MS analysis during the long time of run. Simple visual inspection of the chromatograms found that the predominant urinary compounds consistently in common to SD and Wistar rats were the tricarboxylic acid (TCA) cycle intermediates (succinic acid, aconitic acid, and citric acid), fatty acids (suberic acid and stearic acid), amino acids (glycine, lysine, tyrosine, and tryptophan), and aromatic compounds (*p*-cresol, 4-ethylphenol, hippuric acid, phenylacetylglycine, benzoic, 4-hydroxyphenylacetic, 3-hydroxyphenylpropionic, and 3,4-dihydroxylphenylacetic acid). Actually, the inter-individual metabolite variations within the populations with the similar or even the same genotyping and living environment are ubiquitous (Saude et al. 2007). To comprehensively compare the systematic metabolic variations between the two strains of rats, a metabolomic method based on the data generated by GC/MS was applied in this study.

Metabolic response to fasting

Stress affects complicated biochemical regulatory systems, and might result in marked metabolic disruptions and neuropsychiatric symptoms, such as hypertension, gastric ulcer, depression, anxiety, apathy, and gastrointestinal disorders (Teague et al. 2007; Wang et al. 2007, 2009). In this work, an analysis of PCA was firstly carried out. Some abnormal samples were obviously found by performing PCA on each set of urine samples. More outliers were found from both the fasting SD and Wistar rats in metabolism cages on day 1 than from those on day 3, and more outliers were found from the feeding state (*d*5) than the fasting state (*d*3) as well. These outliers

were further validated by comparing with the total ion current chromatograms from the repeated sample preparation and GC/MS analysis, and such outliers were removed in the final analysis.

After removing all outliers, the PCA scores plots are shown in Fig. 2. A marked separation in PCA scores plot was exhibited between the first (*d*1) and third day's (*d*3) urine samples of fasting Wistar rats (Fig. 2d), as well as an obvious separation trend between those of fasting SD rats (Fig. 2a). Holmes et al. (2000) found that no sampling time-related difference existed in either SD rats or Han Wistar rats over the 8 day collection period. Such short intervals of collecting samples in this study should not produce the obvious metabolic difference for laboratory rats. Although the fasting urines were only collected on *d*1 and *d*3, we further examined if the time-related differences existed as also in the control groups of subsequent acute ethanol intervention experiment (experiment II, *d*8, *d*10, and *d*12). PCA scores plots showed that no profile separations were found between different time points from the feeding control groups of whether SD or Wistar rats (Fig. 2c, f). Such result implied that no obvious response to the handling of intragastric administration.

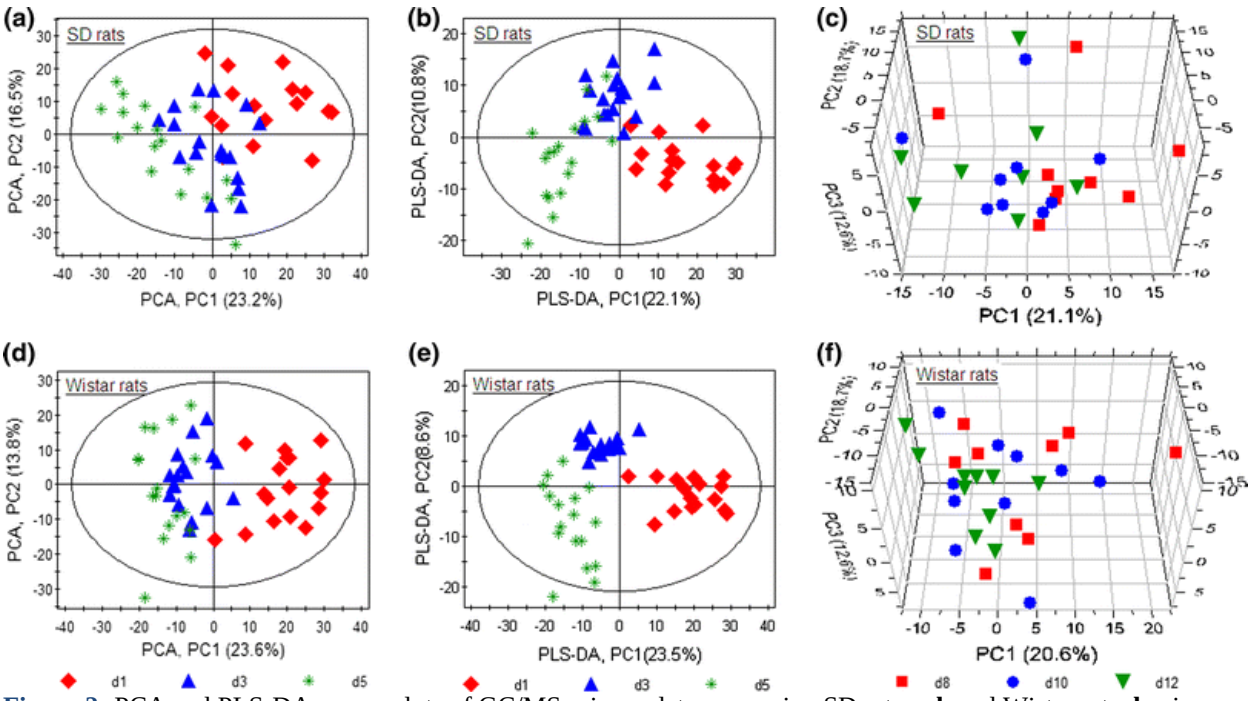

Figure 2: PCA and PLS-DA scores plots of GC/MS urinary data comparing SD rats **a, b** and Wistar rats **d, e** in fasting (*d*1 and *d*3) and feeding state (*d*5), and comparing three consecutive time points of control groups of SD rats **c** and Wistar rats **f** in ethanol intervention. Key: *diamond*, *triangle*, and *star* represent the first (*d*1), third (*d*3), and fifth (*d*5) day of SD or Wistar rats, respectively; *box*, *dot*, and *invert triangle* represent the control samples of first (*d*8), third (*d*10), and fifth (*d*12) ethanol intervention, respectively

PLS-DA was conducted to insight the difference among *d*1 (fasting), *d*3 (fasting), and *d*5 (feeding). Figure 2b, e indicates that the dietary-derived metabolic difference (between *d*3 and *d*5 in PC2) was significantly less than the metabolic difference between *d*1 and *d*3 in PC1. It was presumed that the metabolic response of rats to the abrupt change of living environment in fasting, moving from housing cage to individual metabolism cage on *d*1, might attribute to such

significant profile separation between *d*1 and *d*3. In this work, all rats were housed in standard cage for 1 week before the formal experiment, but they still produced a strong metabolic response to the sudden change in living conditions.

Analysis on the discriminating metabolites between *d*1 and *d*3 indicated that the abrupt environment change and fasting consistently caused the significant decreases of aromatic metabolites (hippuric, 3-hydroxyphenylpropionic, indole-3-acetic, 3-hydroxybenzoic acid, 4-ethylphenol, 1,2-dihydroxybenzene, and *p*-hydroxycinnamic acid), β-alanine, and methylmalonic acid, as well as the marked increases in dicarboxylic acids (malonic, glycolic, adipic, suberic, and nonanedioic acid), long chain fatty acids (palmitic, and stearic acid), aromatic metabolites (4-hydroxybenzoic, 4-hydroxyphenylacetic acid, and phenylacetylglycine), and amino acids (proline and alanine) in both strains. It was reported that the changes of aromatic metabolites are closely correlated to the activity of gut microflora (Gonthier et al. 2003; Phipps et al. 1998). The up-regulated short-chain dicarboxylic acids and long chain fatty acids showed an increasing pressure on energy utilization from the catalysis of fatty acid pathway in fasting. It prompts that the sudden change of living environment not only affected strongly the metabolism of experimental animals, but also provoked a concomitant adjustment on the symbiotic gut microflora. Therefore, both SD and Wistar rats produced a notable fasting-dependent metabolic response.

Metabolomic variations between SD and Wistar rats in fasting and feeding states

To visually profile the two strains of rats, PCA was carried out on the samples without outliers. The PCA scores plots show that SD and Wistar rats are well separated on *d*1 (Fig. 3a) and *d*3 (Fig. 3b) while fasting, as well as a profile separation between SD and Wistar rats in the feeding state (*d*5, Fig. 3c). The model qualities of all PCA are good based on the R^2X values larger than 0.6, and also the representative T-predicted PCA scores plot of feeding rats (Fig. 3d) illustrates the good predictive ability of current model, which can be served to explain the main differences between groups. Thus, a significant physiological disparity is exhibited between SD and Wistar rats.

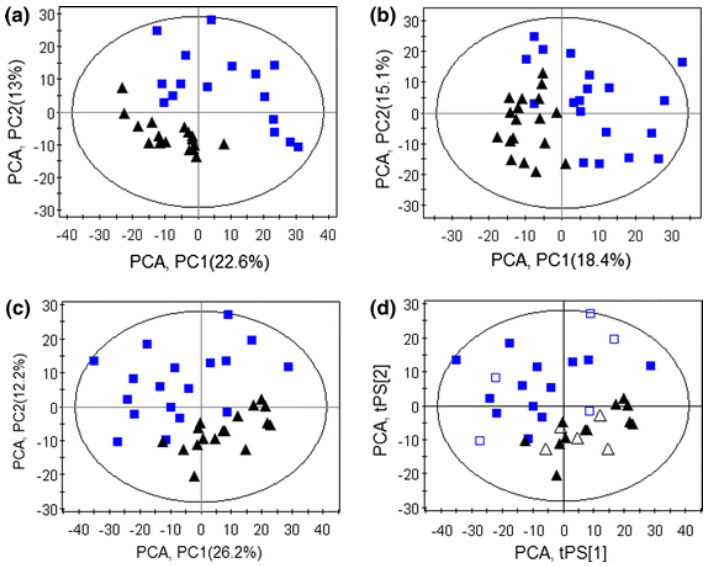

Figure 3: Scores plots of PCA on nocturnal urinary GC/MS data between SD and Wistar rats in fasting and feeding states. **a** Fasting SD rats (*n* = 16) versus fasting Wistar rats (*n* = 17) on *d*1; **b** fasting SD rats (*n* = 19) versus fasting

Wistar rats (n = 18) on d3; **c** feeding SD rats (n = 18) versus Wistar rats (n = 17) on d5; and **d** T-predicted PCA scores plot between feeding SD rats and feeding Wistar rats. Key: *box* SD rats, *triangle* Wistar rats, *square* predicted SD rats, *open triangle* predicted Wistar rats

Distinguishing metabolites of SD and Wistar rats while fasting or feeding

To identify the crucial metabolites responsible for these profile separations from urine metabolome, the compounds with VIP value larger than 1 as determined by OPLS-DA and *P* value of student's *t* test less than 0.05 were selected as discriminating compounds, as summarized in Table 1. In the fasting state, Wistar rats excreted more succinic acid and amino acids such as lysine, pyroglutamic acid, and *N*-acetylaspartic acid, whereas SD rats excreted more aromatic metabolites. When two kinds of rats were fed the same foodstuff, Wistar rats excreted markedly more succinic acid and citric acid, and less aromatic metabolites compared with SD rats.

Table 1: The differential metabolites between nocturnal urines of SD and Wistar rats in fasting (d3) and feeding states (d4)

Compound	Fasting (Wistar vs. SD)		Feeding (Wistar vs. SD)	
	***P*-value (*t*-test)**	**Fold**	***P*-value (*t*-test)**	**Fold**
Ethylmalonic acid[a]	1.24×10^{-5}	−0.334	1.38×10^{-3}	−0.282
Methylsuccinic acid[a]	9.50×10^{-4}	−0.119	–	–
2-Aminopimelic acid	6.90×10^{-3}	−0.275	6.84×10^{-3}	−0.270
Palmitic acid[a]	4.51×10^{-4}	−0.185	–	–
Stearic acid[a]	6.49×10^{-4}	−0.169	–	–
Glycine[a]	1.52×10^{-6}	−0.326	2.57×10^{-3}	−0.246
N-acetylleucine	7.50×10^{-6}	−0.392	6.09×10^{-6}	−0.312
4-Ethylphenol[a]	3.83×10^{-3}	−0.287	1.19×10^{-3}	−0.466
Benzoic acid[a]	1.58×10^{-3}	−0.636	1.86×10^{-3}	−0.415
2-Hydroxybenzoic acid[a]	–	–	1.82×10^{-2}	−0.211
4-Hydroxyphenylacetic acid[a]	7.55×10^{-3}	−0.113	7.46×10^{-2}	−0.077
2-Hydroxyphenylpropionic acid	3.38×10^{-3}	−0.226	1.46×10^{-2}	−0.226
3-Hydroxyphenylpropionic acid[a]	–	–	3.47×10^{-2}	−0.139
Indole-3-acetic acid[a]	–	–	4.37×10^{-2}	−0.149
4-Hydroxyphenylpropionic acid[a]	–	–	1.61×10^{-2}	−0.105
Homovanillic acid[a]	–	–	2.55×10^{-2}	−0.108
3,4-Dihydroxyphenylacetic acid[a]	1.95×10^{-4}	−0.133	–	–
3,4-Dihydroxyphenylpropionic acid[a]	6.80×10^{-10}	−0.486	1.08×10^{-3}	−0.275
Methylmalonic acid[a]	7.33×10^{-5}	0.371	–	–
Succinic acid[a]	1.70×10^{-5}	0.269	4.32×10^{-3}	0.193
Citric acid[a]	–	–	7.38×10^{-3}	0.149
Pyroglutamic acid[a]	1.93×10^{-3}	0.139	–	–
Lysine[a]	1.57×10^{-2}	0.131	–	–
N-acetylaspartic acid	3.76×10^{-4}	0.227	–	–
Proline[a]	–	–	1.79×10^{-3}	0.191
Phenylacetylglycine	–	–	4.81×10^{-3}	0.122
4-Methylphenol[a]	4.30×10^{-4}	0.302	3.42×10^{-3}	0.296

[a]These compounds were validated by reference standard substances

In this work, PCA revealed an obvious metabolic separation between the two strains in both fasting and feeding states. The discriminating metabolites indicated that the main distinctions between two strains were caused by fatty acids, amino acids, and aromatic compounds (Table 1). Previous reports indicated that metabolic disorder of fatty or branch-chain amino acids in mitochondria usually caused the accumulation of a large amount of methylmalonic or ethylmalonic acid in tissues and biofluids (Nowaczyk et al. 1998; Ozand et al. 1994). Current work indicated clearly that Wistar rats produced higher levels of methylmalonic and succinic acid in pairs than SD rats. Mirandola et al.'s (2008) work demonstrated that methylmalonic acid

inhibited the oxidation of succinic acid in mitochondria, and hence higher concentrations of succinic acid were excreted together with methylmalonic acid in the urines of fasting Wistar rats compared to the fasting SD rats. Additionally, it was interesting to find that ethylmalonic and methylsuccinic acids were both significantly higher in SD rats rather than Wistar rats in the fasting condition, suggesting that the SD rats probably produced higher levels of metabolites relating to ethylmalonic encephalopathy than Wistar rats (Nowaczyk et al. 1998). We deduced that, in starvation, the metabolic disorder of fatty or branch-chain amino acids took place with significant difference between SD and Wistar rats.

As the scores plot shown in Fig. 3, SD rats exhibited a significantly higher inter-individual metabolic variation (more scattered profile) than Wistar rats (more compacted profile). The discriminating metabolites analysis indicated that more urinary aromatic metabolites were detected in SD rats than in Wistar rats in fasting state, and the feeding further promoted the excretion of more aromatic metabolites in SD rats compared with Wistar rats (Table 1). It is known that phenolic acids are usually correlated with metabolism of aromatic amino acids and dietary phenolics under the transformation of gut microflora (Gonthier et al. 2003; Jacobs et al. 2009; Phipps et al. 1998). We supposed that such inter-individual variation within strain probably was related to their symbiotic gut microflora, which was considered as an external factor closely affecting metabolic profile. Herein, gut microflora possibly play a greater role on SD rats than Wistar rats. It is known that some oral drugs and food components usually experience degradation, transformation, or detoxification by gut microbes before being absorbed. Thus, such differences between different strains of experimental animals should be considered when performing researches at animal level.

Metabolomic variations caused by acute ethanol intervention

The fed rats were selected in the subsequent experiments of acute ethanol intervention, with the following two reasons, (1) the similar profile separation between SD and Wistar rats in the feeding state to that in the fasting state (see section “3.3”, Fig. 3); (2) in contrast to the fasting, the feeding can effectively decrease the death of rats during ethanol administration according to preliminary experiment. Although no profile separation was observed in PC1 and PC2 of PCA scores plot between the control groups of SD and Wistar rats after the first day’s ethanol intervention (*d*8) (figure not shown), the clear separation appeared in PC2 and PC4 of PCA scores plot (Fig. 4a). Likewise, a clear profile separation between the control groups of SD and Wistar rats was only present in the PC1 and PC4 of PCA scores plot after the third day’s ethanol intervention (Fig. 4b) or in the PC2 and PC3 of that after the fifth day’s ethanol intervention (Fig. 4c). In spite of the decreasing ability of profile separation in PCA scores plot, current works shows that the metabolic differences were indeed present between two strains of control rats, as is similar to that in normal physiological condition (see Fig. 2c).

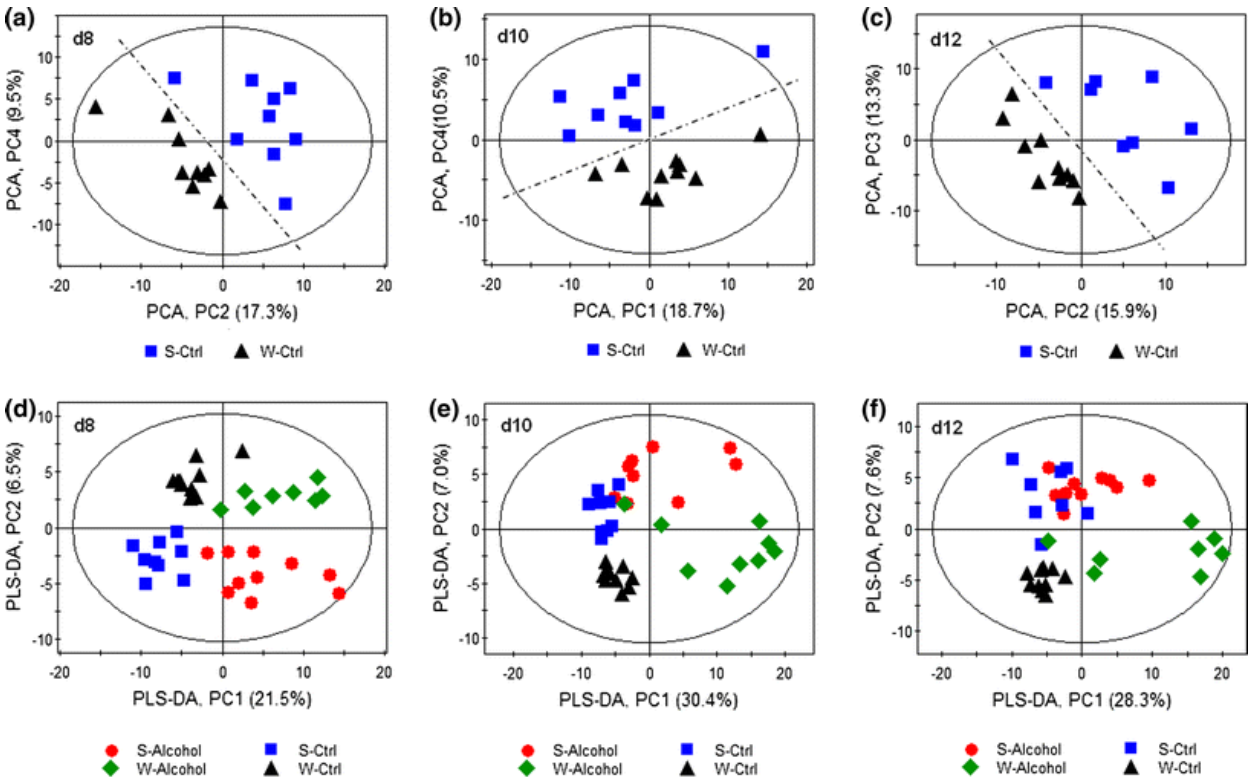

Figure 4: Scores plots of SD and Wistar rats by the consecutive ethanol exposure (*d*8, *d*10, *d*12). **a**–**c** the comparison of the control groups between SD and Wistar rats in three repeated ethanol intervention (PCA); **d**–**f** the comparison between the control group and ethanol group of SD rats and Wistar rats (PLS-DA). Key: *dot* ethanol SD rat, *box* control SD rat, *diamond* ethanol Wistar rat, and *triangle* control Wistar rat

In order to reduce noise disturbance, PLS-DA was performed to evaluate the effects of ethanol intervention on the metabolic profiles of rats. Figure 4d shows that the first acute ethanol intervention (*d*8) caused a significantly changed urinary metabolite profile whether for SD rats or Wistar rats. It was further found that the ethanol group and control group of SD rats tended to overlap on the scores plot of PLS-DA after the third repeated ethanol intervention (*d*10, Fig. 4e), and such trend was further strengthened after the fifth repeated ethanol intervention (*d*12, Fig. 4f). This result implied that SD rats possibly have a powerful capability of self-adjustment to the repeated ethanol administration. Figure 4d also demonstrates that the first acute ethanol intervention on Wistar rats resulted in an obvious profile separation from their control group on the scores plot of PLS-DA, and such separation was kept or even strengthened following the third (Fig. 4e) and fifth (Fig. 4f) repeated ethanol administrations. Therefore, SD rats and Wistar rats showed a different metabolic response to the consecutive ethanol administration, where SD rats supposedly exhibited a better capacity of self-adjustment to the repeated ethanol intervention than Wistar rats.

Changes of blood and liver biochemical parameters cause by consecutive acute ethanol intervention

Oxidative stress and reactive oxygen species mediated toxicity are considered the key underlying mechanisms responsible for ethanol-induced liver injury and mitochondrial dysfunction (Cederbaum et al. 2009; Haorah et al. 2008). The activities of three principal plasma

transaminases, ALT, AST, and LDH, will significantly increase and are generally the most sensitive indexes in the diagnosis of hepatic diseases. The results indicate that 5 days of repeated ethanol exposure caused the elevated activities of AST and LDH of Wistar rats with high significance ($P < 0.01$). Meanwhile, the levels of AST and ALT of SD rats were significantly enhanced ($P < 0.05$; Table 2). Such changes of biochemical parameters indicated that Wistar rats probably underwent more hepatic injury than SD rats in the procedure of ethanol intervention.

Table 2: Biochemical parameters of serum (ALT, AST, and LDH) and liver (LPO, GSH-PX, and SOD) of ethanol rats and control rats after five consecutive ethanol interventions

Parameters	SD rats		Wistar rats	
	Control	Ethanol	Control	Ethanol
AST	175 ± 21	218 ± 44*	182 ± 23	232 ± 30**
ALT	48.1 ± 8.5	57.3 ± 9.7*	62.4 ± 4.1	64.9 ± 7.5
LDH	1,446 ± 296	1,505 ± 264	1,783 ± 314	2,248 ± 226**
LPO	1.035 ± 0.410	1.178 ± 0.564	1.340 ± 0.925	1.113 ± 0.431
SOD	252 ± 42	218 ± 35	259 ± 56	203 ± 50*
GSH-PX	2,832 ± 730	2,652 ± 615	3,718 ± 862	2,448 ± 454**

* Significant difference statistically between control group and ethanol group ($P < 0.05$)
** Highly significant difference statistically between control group and ethanol group ($P < 0.01$)

The activities of SOD ($P < 0.05$) and GSH-PX ($P < 0.01$) in Wistar rats were significantly decreased by ethanol administration (Table 2). However, no significant decreases of these two enzymes in SD rats were observed. SOD is a basic protective enzyme responsible for dismuting reactive oxygen radical to hydrogen peroxide and oxygen. The decreased SOD activity results in the accumulation of these highly reactive free radicals, ultimately leading to the oxidative metabolism dysfunction, cell injury and biochemical metabolism disorder. GSH is a major non-protein thiol that plays a central role in coordinating the antioxidant defense process. GSH metabolizes hydrogen peroxide to water, thereby protects mammalian cells against oxidative damage (Reddy et al. 2009). This experiment showed that ethanol might decrease the ability of removing reactive oxygen radical of Wistar rats. LPO level is normally increased significantly in the liver of ethanol hepatopathy, and indirectly indicates the degree of cell injury from free radical attack. In this study, LPO levels were not significantly changed in both strains of rats in statistics, but the hepatic LPO level of Wistar rats was indeed increased in average value. High inter-individual variability of LPO levels within Wistar rats decreased the statistical significance. The change of above biochemical parameters on serum and tissue implied that Wistar might have hypersensitivity to ethanol exposure and suffer more hepatic injury than SD rats.

Discriminating metabolites and changes of biochemical pathways caused by consecutive acute ethanol intervention

In fact, the time-related quantity changes of discriminating metabolite between SD and Wistar rats exposed to repeated ethanol intervention indicated that the first acute ethanol intervention caused approximately the same number of differentially expressed urinary metabolites for both SD and Wistar rats (Fig. 5a). The consecutive ethanol intervention significantly increased the quantity of discriminating metabolites between Wistar ethanol and control group, while the quantity decreased in the SD rats, suggesting the different capacities of self-adjustment to exogenous intervention. Additionally, this finding showed that the initial several times of outcomes might be also out of consideration when performing a rigorous animal experiment. To obtain the reliable and high weighting of discriminating metabolites, the results of the fifth

ethanol exposure from UV-scaled OPLS–DA models were further validated by Pareto-scaled OPLS–DA models, and as a result the reduced discriminating metabolites were structurally validated (Fig. 5b).

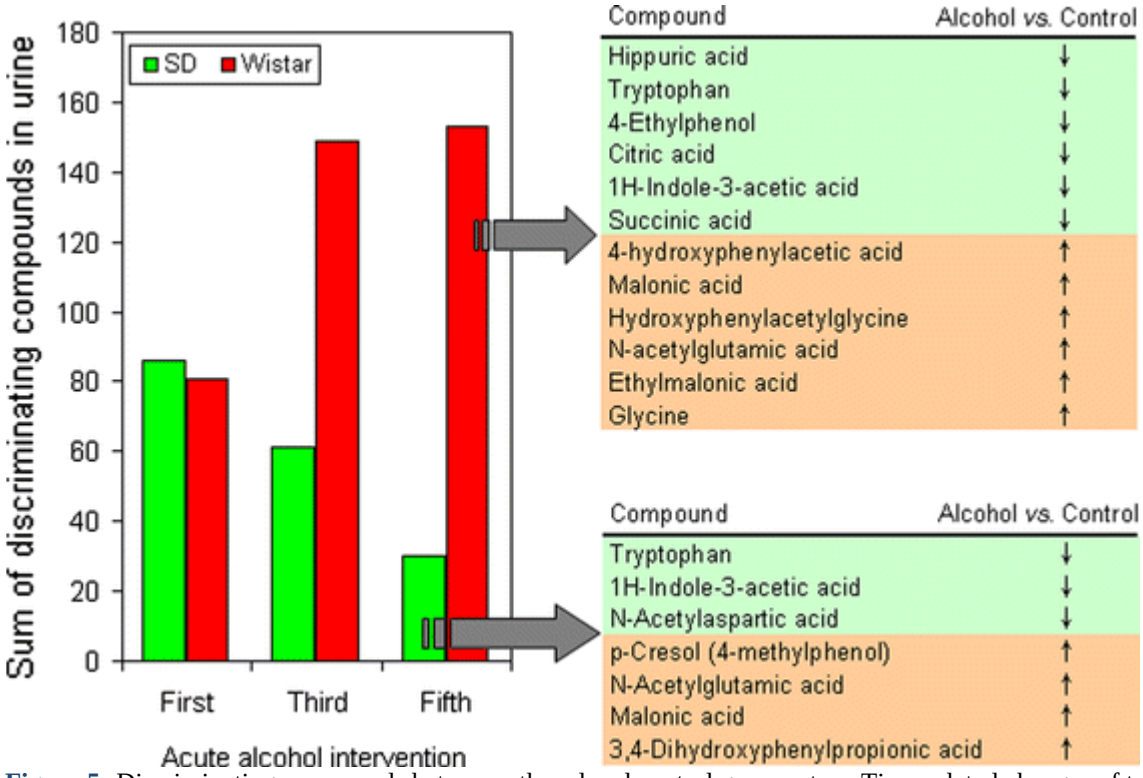

Figure 5: Discriminating compounds between ethanol and control group rats. **a** Time-related changes of total discriminating compounds by Student's *t* test and UV-scaled OPLS-DA model (SD rats: 1 principal component, $R^2X = 0.159$, $R^2Y = 0.683$, $Q^2 = 0.279$; Wistar rats: 1 principal component, 1 orthogonal component, $R^2X = 0.512$, $R^2Y = 0.909$, $Q^2 = 0.676$), and **b** the main discriminating compounds obtained by the further Pareto-scaled OPLS-DA models (SD rats: 1 principal component, 1 orthogonal component, $R^2X = 0.322$, $R^2Y = 0.814$, $Q^2 = 0.455$; Wistar rats: 1 principal component, $R^2X = 0.602$, $R^2Y = 0.685$, $Q^2 = 0.649$)

It was found that ethanol intervention changed the metabolism of short-chain dicarboxylic acids, TCA cycle, amino acids, and aromatic compounds. Ethanol-induced oxidative stress and mitochondrial dysfunction probably result in oxidation disorder of short chain fatty acids or branch chain amino acids, and thereby such disorders prevents the body from converting short chain fatty acids into energy (Bok et al. 2003; Jethva et al. 2008). The significantly elevated malonic acid and ethylmalonic acid in ethanol group of Wistar rats indicated that they suffered more hepatic injury than the ethanol group of SD rats. Hippuric acid, as the conjugated product of benzoic acid with glycine in liver, is correlated to polyphenols ingestion, principally caused by gut microflora, and liver function. In ethanol group of Wistar rats, the increased urinary contents of glycine and benzoic acid ($P = 0.16$, no univariate statistical significance), and the decreased hippuric acid suggested a metabolic dysfunction of damaged liver.

Some distinguishing aromatic metabolites are well known gut microbial cometabolites (Chamkha et al. 2001; Li et al. 2008). Figure 5b indicates that ethanol caused a distinct

expression of *p*-cresol, 4-ethylphenol, 4-hydroxyphenylacetic acid, 3,4-dihydroxyphenylpropionic acid, and 4-hydroxyphenylacetylglycine in both two strains, probably suggesting a changed structure of gut microflora. Additionally, the different alterations of these compounds in two strains under ethanol intervention, such as the elevated *p*-cresol only in ethanol group of SD rats and the decreased 4-ethylphenol just in ethanol group of Wistar rats compared with control group, respectively, might suggest a differential restructuring of symbiotic gut microflora between two strains.

Simultaneously, there were also some consistent results between ethanol-induced SD and Wistar rats. According to the reported findings that chronic ethanol ingestion disturbs the metabolism of tryptophan in male Wistar rats (Bonner et al. 1993), our results also proved the coincidental reduction of the urinary tryptophan and indole-3-acetic acid in both ethanol groups of SD and Wistar rats compared with their control groups.

In conclusion, GC/MS-based metabolomic analysis reveals the subtle metabotype differences between the two strains of commonly used laboratory rats, SD and Wistar rats, in fasting, feeding, and ethanol intervention. Both strains demonstrated a strong response to the abrupt environmental perturbations, resulting in metabolomic changes of rats and the concomitant changes of symbiotic gut microflora. The fasting condition resulted in the differential expression of fatty acids and branch-chain amino acids between the two strains of rats, including a higher level of methylmalonic acid and a lower level of ethylmalonic acid in Wistar rats than SD rats. The repeated ethanol intervention experiments revealed different time-dependent metabolic responses between the two strains. In contrast to Wistar rats, SD rats exhibited a better ability of self-recovery which led to a weaker hepatic injury from the consecutive ethanol exposure based on the results from the urinary metabolomic analysis and the biochemical markers of blood and liver samples. In summary, GC/MS-based metabolomics provides new insight into the intrinsic metabolic differences between SD and Wistar rats upon perturbations such as fasting, feeding states and ethanol exposure, which warrant a thorough consideration in experimental design as well as data interpretation for pharmacological and nutritional investigations. The same -omics strategy can be utilized to establish correlation between metabotypes of different animal strains and those among human populations that will eventually facilitate the translation of animal data to human clinical endpoints.

ABBREVIATIONS

ALT	Alanine aminotransferase
AST	Aspartate aminotransferase
GC/MS	Gas chromatography coupled to mass spectrometry
GSH-PX	Glutathione peroxidase
IS	Internal standard
LDH	Lactate dehydrogenase
LPO	Lipid peroxidation
NMR	Nuclear magnetic resonance
OPLS–DA	Orthogonal projections to latent structures discriminant analysis
PCA	Principal component analysis
SD rats	Sprague–Dawley rats
SOD	Superoxide dismutase

UV	Unite variance
VIP	Variable influence on projection

ACKNOWLEDGMENTS

This work was financially supported by the projects of Shanghai Commission of Science and Technology (07DZ19715), and National comprehensive technology platforms for innovative drug R&D (2009ZX09301-007) and E-institutes of Shanghai Municipal Education Comminssion, Project Number: E03008, 09YZ119.

REFERENCES

Bok, L. A., Vreken, P., Wijburg, F. A., et al. (2003). Short-chain acyl-CoA dehydrogenase deficiency: Studies in a large family adding to the complexity of the disorder. *Pediatrics, 112*, 1152–1155.

Bollard, M. E., Holmes, E., Lindon, J. C., et al. (2001). Investigations into biochemical changes due to diurnal variation and estrus cycle in female rats using high-resolution H-1 NMR spectroscopy of urine and pattern recognition. *Analytical Biochemistry, 295*, 194–202.

Bollard, M. E., Stanley, E. G., Lindon, J. C., Nicholson, J. K., & Holmes, E. (2005). NMR-based metabonomic approaches for evaluating physiological influences on biofluid composition. *NMR in Biomedicine, 18*, 143–162.

Bonner, A. B., Brien, S., & Preedy, V. R. (1993). The urinary-excretion of tryptophan and tryptophan-metabolites in the chronic ethanol-fed rat. *Journal of Pharmacy and Pharmacology, 45*, 81–85.

Bylesjö, M., Rantalainen, M., Cloarec, O., Nicholson, J. K., Holmes, E., & Trygg, J. (2006). OPLS discriminant analysis: combining the strengths of PLS-DA and SIMCA classification. *Journal of Chemometrics, 20*, 341–351.

Cederbaum, A. I., Lu, Y. K., & Wu, D. F. (2009). Role of oxidative stress in alcohol-induced liver injury. *Archives of Toxicology, 83*, 519–548.

Chamkha, M., Garcia, J. L., & Labat, M. (2001). Metabolism of cinnamic acids by some Clostridiales and emendation of the descriptions of *Clostridium aerotolerans*, *Clostridium celerecrescens* and *Clostridium xylanolyticum*. *International Journal of Systematic and Evolutionary Microbiology, 51*, 2105–2111.

Gao, X., Pujos-Guillot, E., Martin, J.-F., et al. (2009). Metabolite analysis of human fecal water by gas chromatography/mass spectrometry with ethyl chloroformate derivatization. *Analytical Biochemistry, 393*, 163–175.

Gonthier, M. P., Cheynier, V., Donovan, J. L., et al. (2003). Microbial aromatic acid metabolites formed in the gut account for a major fraction of the polyphenols excreted in urine of rats

fed red wine polyphenols. *Journal of Nutrition, 133*, 461–467.

Haorah, J., Ramirez, S. H., Floreani, N., Gorantla, S., Morsey, B., & Persidsky, Y. (2008). Mechanism of alcohol-induced oxidative stress and neuronal injury. *Free Radical Biology and Medicine, 45*, 1542–1550.

Holmes, E., Nicholls, A. W., Lindon, J. C., et al. (2000). Chemometric models for toxicity classification based on NMR spectra of biofluids. *Chemical Research in Toxicology, 13*, 471–478.

Jacobs, D. M., Gaudier, E., van Duynhoven, J., & Vaughan, E. E. (2009). Non-digestible food ingredients, colonic microbiota and the impact on gut health and immunity: A role for metabolomics. *Current Drug Metabolism, 10*, 41–54.

Jethva, R., Bennett, M. J., & Vockley, J. (2008). Short-chain acyl-coenzyme A dehydrogenase deficiency. *Molecular Genetics and Metabolism, 95*, 195–200.

Jiye, A., Trygg, J., Gullberg, J., et al. (2005). Extraction and GC/MS analysis of the human blood plasma metabolome. *Analytical Chemistry, 77*, 8086–8094.

Lenz, E. M., & Wilson, I. D. (2007). Analytical strategies in metabonomics. *Journal of Proteome Research, 6*, 443–458.

Li, M., Wang, B. H., Zhang, M. H., et al. (2008). Symbiotic gut microbes modulate human metabolic phenotypes. *Proceedings of the National Academy of Sciences of the United States of America, 105*, 2117–2122.

Lin, J. C., Su, M. M., Wang, X. Y., et al. (2008). Multiparametric analysis of amino acids and organic acids in rat brain tissues using GC/MS. *Journal of Separation Science, 31*, 2831–2838.

McKee, C. L. G., Wilson, I. D., & Nicholson, J. K. (2006). Metabolic phenotyping of nude and normal (Alpk : ApfCD, C57BL10J) mice. *Journal of Proteome Research, 5*, 378–384.

Mirandola, S. R., Melo, D. R., Schuck, P. F., Ferreira, G. C., Wajner, M., & Castilho, R. F. (2008). Methylmalonate inhibits succinate-supported oxygen consumption by interfering with mitochondrial succinate uptake. *Journal of Inherited Metabolic Disease, 31*, 44–54.

Nowaczyk, M. J. M., Lehotay, D. C., Platt, B. A., et al. (1998). Ethylmalonic and methylsuccinic aciduria in ethylmalonic encephalopathy arise from abnormal isoleucine metabolism. *Metabolism—Clinical and Experimental, 47*, 836–839.

Ozand, P. T., Rashed, M., Millington, D. S., et al. (1994). Ethylmalonic aciduria: an organic acidemia with CNS involvement and vasculopathy. *Brain and Development, 16*, 12–22.

Phipps, A. N., Stewart, J., Wright, B., & Wilson, I. D. (1998). Effect of diet on the urinary excretion of hippuric acid and other dietary-derived aromatics in rat. A complex interaction between diet, gut microflora and substrate specificity. *Xenobiotica, 28*, 527–537.

Plumb, R. S., Granger, J. H., Stumpf, C. L., et al. (2005). A rapid screening approach to metabonomics using UPLC and oa-TOF mass spectrometry: application to age, gender and diurnal variation in normal/Zucker obese rats and black, white and nude mice. *Analyst, 130*, 844–849.

Potts, B. C. M., Deese, A. J., Stevens, G. J., Reily, M. D., Robertson, D. G., & Theiss, J. (2001). NMR of biofluids and pattern recognition: assessing the impact of NMR parameters on the principal component analysis of urine from rat and mouse. *Journal of Pharmaceutical and Biomedical Analysis, 26*, 463–476.

Psihogios, N. G., Gazi, I. F., Elisaf, M. S., Seferiadis, K. I., & Bairaktari, E. T. (2008). Gender-related and age-related urinalysis of healthy subjects by NMR-based metabonomics. *NMR in Biomedicine, 21*, 195–207.

Qiu, Y., Su, M., Liu, Y., et al. (2007). Application of ethyl chloroformate derivatization for gas chromatography-mass spectrometry based metabonomic profiling. *Analytica Chimica Acta, 583*, 277–283.

Reddy, V. D., Padmavathi, P., & Varadacharyulu, N. C. (2009). Emblica officinalis protects against alcohol-induced liver mitochondrial dysfunction in rats. *Journal of Medicinal Food, 12*, 327–333.

Salek, R. M., Maguire, M. L., Bentley, E., et al. (2007). A metabolomic comparison of urinary changes in type 2 diabetes in mouse, rat, and human. *Physiological Genomics, 29*, 99–108.

Saude, E. J., Adamko, D., Rowe, B. H., Marrie, T., & Sykes, B. D. (2007). Variation of metabolites in normal human urine. *Metabolomics, 3*, 439–451.

Slupsky, C. M., Rankin, K. N., Wagner, J., et al. (2007). Investigations of the effects of gender, diurnal variation, and age in human urinary metabolomic profiles. *Analytical Chemistry, 79*, 6995–7004.

Teague, C. R., Dhabhar, F. S., Barton, R. H., et al. (2007). Metabonomic studies on the physiological effects of acute and chronic psychological stress in Sprague-Dawley rats. *Journal of Proteome Research, 6*, 2080–2093.

Wang, X. Y., Su, M. M., Qiu, Y. P., et al. (2007). Metabolic regulatory network alterations in response to acute cold stress and ginsenoside intervention. *Journal of Proteome Research, 6*, 3449–3455.

Wang, X. Y., Zhao, T., Qiu, Y. P., et al. (2009). Metabonomics approach to understanding acute and chronic stress in rat models. *Journal of Proteome Research, 8*, 2511–2518.

Want, E. J., Nordstrom, A., Morita, H., & Siuzdak, G. (2007). From exogenous to endogenous: The inevitable imprint of mass spectrometry in metabolomics. *Journal of Proteome Research, 6*, 459–468.

Wikoff, W. R., Anfora, A. T., Liu, J., et al. (2009). Metabolomics analysis reveals large effects of gut microflora on mammalian blood metabolites. *Proceedings of the National Academy of Sciences of the United States of America, 106*, 3698–3703.